

The spatial and temporal evolution of the deep water in the Arctic Ocean's Canada Basin

Catherine Zhang

Advisor: Mary-Louise Timmermans

Second Reader: David Evans

December 13, 2023

A Senior Thesis presented to the faculty of the Department of Earth and Planetary Sciences, Yale University, in partial fulfillment of the Bachelor's Degree.

In presenting this thesis in partial fulfillment of the Bachelor's Degree from the Department of Earth and Planetary Sciences, Yale University, I agree that the department may make copies or post it on the departmental website so that others may better understand the undergraduate research of the department. I further agree that extensive copying of this thesis is allowable only for scholarly purposes. It is understood, however, that any copying or publication of this thesis for commercial purposes or financial gain is not allowed without my written consent.

Catherine Zhang, 13 December, 2023

Abstract

The deep water of the Canada Basin (CB) has been isolated for approximately 500 years and is the oldest water in the Arctic Ocean, providing an opportunity to study past Arctic climate and predict future changes in Arctic circulation. Many studies have aimed to explain the ventilation rates and heat fluxes in the CB deep water using temperature and salinity observational and theoretical approaches, but little has been done using dissolved oxygen data. In this study, we use dissolved oxygen data in conjunction with temperature and salinity data from 2003-2022 annual icebreaker cruises to examine spatial and temporal changes in the CB deep water. Spatially, the CB deep water is homogenous throughout the center of the basin but increases in temperature and decreases in dissolved oxygen near the shelves. Temporally, the CB deep water is warming at a rate of $\sim 0.0003^{\circ}\text{C yr}^{-1}$, decreasing in dissolved oxygen, decreasing in salinity in the upper portion of the CB deep water, and experiencing a decrease in total thickness of the layer. Together, these results are consistent with claims that the CB deep water experiences no ventilation, stores geothermal heat that travels vertically upward from the basin floor, and may be experiencing the effects of changing gyre dynamics.

1 Introduction

The Canada Basin (CB) is one of the main deep basins in the Arctic Ocean. It has a depth of around 4000 m and is separated from the Eurasian Basin by the Lomonosov Ridge with sill depth around 2000 m, limiting deep-water exchange and isolating the deep waters of the CB. The effects of this bathymetric feature, along with other inputs higher in the water column, is reflected in the thermohaline structure that is consistent throughout the CB. Starting at the surface and increasing in depth, the structure begins with a relatively fresh layer (the Polar Mixed Layer) until ~ 50 m, which is then followed by a strongly salt-stratified layer of Pacific origins to 400 m depth (Timmermans et al., 2004; Timmermans et al., 2018). A warmer layer with origins from the Atlantic sits between around 400 to 1500 m, after which the water temperature decreases with depth until a local potential temperature minimum (T_{\min}). The CB deep water is defined to start at the potential temperature minimum at around 2400 m depth, and from 2400 to 2700 m, analysis of potential temperature and salinity data show a double diffusive staircase structure (indicating laterally-coherent layers) before temperature and salinity stay constant from 2700 m to the bottom in a homogeneous bottom layer (henceforth the CB bottom water) (Timmermans et al., 2003). This bottom layer has not been ventilated for approximately

500 years (Schlosser et al., 1997; Timmermans et al., 2003), making the CB deep water the oldest water in the Arctic Ocean.

The age of the CB deep water provides a unique opportunity to study past Arctic climate and predict future changes in Arctic circulation. Thus, there have been many studies focusing on the present evolution of the CB deep water, specifically on the topics of ventilation rates and heat flows. A study by Aagard et al. (1985) stated that the CB deep water is ventilated slowly through brine rejection on the shelves or from in-fluxes from the Eurasian Basin. In contrast, a study by Timmermans et al. (2003) assumed a no ventilation scenario and used observational data and theoretical calculations to demonstrate how geothermal heat escapes laterally through the edges of the basin. On the other hand, Carmack et al. (2012), using observational data, show a CB bottom water warming rate of $\sim 0.0004^{\circ}\text{C yr}^{-1}$ and no salinity change, consistent with a scenario of no ventilation (like conclusions drawn by Aagaard & Carmack, 1994) and geothermal heat being stored and flowing vertically up through the CB deep water.

One unexamined parameter in the CB deep water literature is dissolved oxygen. The oxygen concentrations of water reflect the surface conditions when the water was last in contact with the atmosphere and are slowly modified by changing physical factors (like temperature) and biogeochemical factors (such as photosynthesis and respiration) below the surface (Arroyo et al., 2023). These factors make oxygen concentration an effective tool when measuring ventilation rates. In this study, we extend the work of Carmack et al. (2012) by adding dissolved oxygen concentration to our analysis of potential temperature and salinity and examining trends across the basin from 2003 to 2022. Our analysis aims to describe spatial and temporal changes in the CB deep water and to add to our understanding of heat flows and ventilation pathways in the basin.

2 Data and Methods

2.1 Data

This thesis used 2003-2022 data from annual hydrographic surveys conducted from the *Canadian Coast Guard Ship Louis S. St-Laurent* JOIS/BGOS program. Annual survey data, collected sometime between the months July and October, records a variety of physical and biogeochemical processes at each station, but only temperature, salinity, dissolved oxygen, pressure, and depth data are used for this study. Hydrographic profile data were collected at each

station using a 24-bottle rosette with a Seabird CTD with oxygen (SBE-43), fluorescence, and transmission sensors. Temperature sensors were calibrated yearly, and conductivity and oxygen sensor data were calibrated using bottle measurements as outlined in McLaughlin et al. (2008). The precision of the sensors are: pressure = 1.4 db, temperature = 0.001°C, salinity = 0.001, and oxygen = 0.05 mL L⁻¹.

2.2 Defining sections

To examine the spatial evolution of the CB, we defined four different sections over the years from 2003 to 2022 (Fig. 1). These sections closely followed the four interlocking sections upon which the *CCGS Louis S. St-Laurent* conducted surveys and were chosen to maximize the number of data points per year per section.

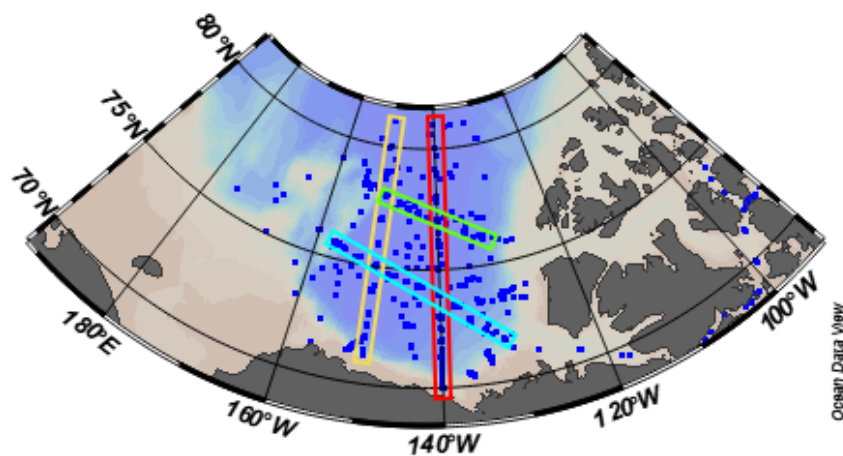


Figure 1. A map displaying all CTD data from the 2003 to 2022 annual icebreaker surveys. The colored rectangles represent the 4 different sections analyzed: along 140°W longitude (red), along 150°W longitude (yellow), a northern E-W section (green), and a southern E-W section (blue).

Section plots were created using potential temperature, salinity, and dissolved oxygen data and were limited to depths between 2200 and 4000 m, which allowed us to observe T_{\min} , the transition layer, and the homogeneous bottom layer. We compared section plots from each year visually, then moved onto more quantitative analysis based on our preliminary observations.

2.2 Defining the extent of CB bottom water and T_{min} location

For all years of cruise data, only casts with depths greater than or equal to 3,000 m were considered. This guaranteed that the locations of accepted casts were near the center of the Canada Basin, the area of interest. The bottom of the CBDW was defined to be 10 m above the lowest extent of each profile, and the top of the CB bottom water was 10m below the point at which the potential temperature exceeds 0.0008°C the temperature at the bottom of the profile. We chose 0.0008°C as the limiting temperature variation based off its consistency in defining the top of the CB bottom water at the top of the homogenous bottom layer. The location of T_{min} was determined by finding the minimum potential temperature location in the bottom half of each cast. If the height of the CB bottom water was less than 50 m, the average thickness of the first layer above the homogenous bottom layer (Timmermans et al., 2003), then the profile was discarded. Fig. 2 shows the location of the casts that were used in our calculations.

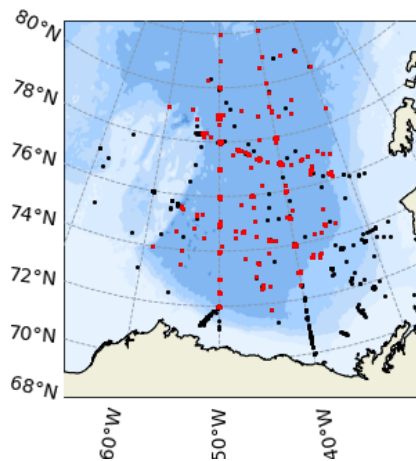


Figure 2. A map showing the locations of all casts from 2003-2022 (all dots), highlighting the casts that satisfy the requirements of a minimum depth of 3000 m and bottom thickness of at least 50 m (red dots).

For the 2015 cruise, a problem was identified with the CTD wire after cast 8; consequently, all following casts were limited to 3000 m in depth. Despite this limitation, the method described above was still used to define the CB bottom water in 2015, and the average values and standard deviation of the CB bottom water in 2015 was found to be comparable to other years of analysis (shown in Fig. 3). Thus, we decided to keep the casts of 2015 in our analysis, except for calculations relating to the thickness of the CB bottom water.

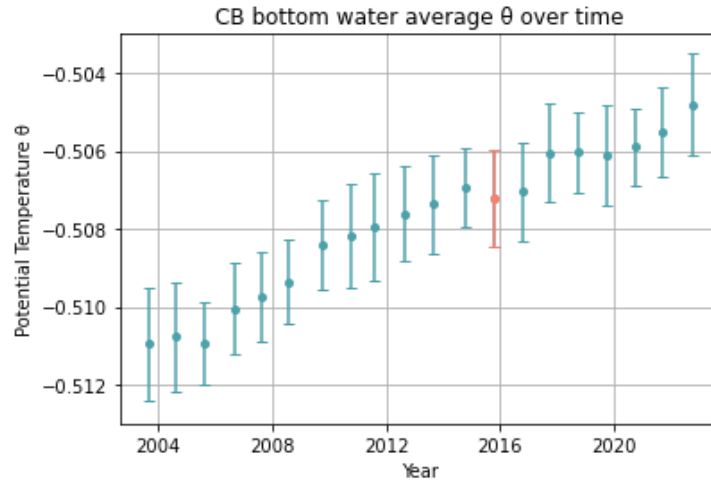


Figure 3. A scatter plot showing average potential temperature of the CB deep water over time. Error bars represent two times the standard deviation. The year 2015 is highlighted in pink.

2.3 Calculating oxygen solubility and apparent oxygen utilization

Oxygen solubility (O_2sol) and Apparent Oxygen Utilization (AOU) are two quantities that can provide insights to the driving mechanisms of dissolved oxygen variations. O_2sol is the concentration of oxygen in water that is in equilibrium with the atmosphere. Here, we calculated O_2sol throughout the water column using temperature, salinity, and pressure with the equations established by Garcia & Gordon (1992). AOU is defined as the difference between O_2sol and in situ dissolved oxygen concentration and was calculated using the following relationship:

$$AOU = O_2sol - O_2$$

Where O_2 is the concentration of dissolved oxygen.

While O_2sol is useful in identifying changes associated with physical properties, AOU is useful in identifying changes associated with biological factors. Since O_2sol is most dependent on temperature and less dependent on salinity and pressure, we expect changes in temperature to be associated with changes in O_2sol . Indeed, higher (lower) O_2sol is associated with colder (warmer) waters. On the other hand, changes in AOU are driven by photosynthesis (producing oxygen) and respiration (consumption of oxygen). Water transport processes also impact AOU: a well-ventilated water mass would have a lower AOU than an isolated one, which has lost more of its oxygen through respiration than has been replenished (Koeve & Kähler, 2016).

2.4 Analysis of temporal changes over specific locations

Three locations were identified for further temporal analysis given the high number of casts around those areas from 2003-2022. Location 1 is defined to be at 77°N, 144°W; location 2 is at 74°N, 140°W; and location 3 is at 75°N, 150°W. For each location, casts were accepted if their latitude and longitude were within one degree of the location definition.

3 Results

3.1 Consistent structure of the CB deep water

Potential temperature and salinity profiles show a distinctive staircase structure followed by a homogenous bottom layer throughout the basin between the years 2003-2022. This trend is also seen in dissolved oxygen profiles, the only difference being that dissolved oxygen concentration decreases with depth. When observed at a single location, profiles are seen to maintain their general shape while undergoing shifts in temperature, salinity, and/or dissolved oxygen (Fig. 4). The details of the structure and how different landmarks (T_{\min} and the CB bottom water) vary spatially and temporally will be expanded upon in the following sections.

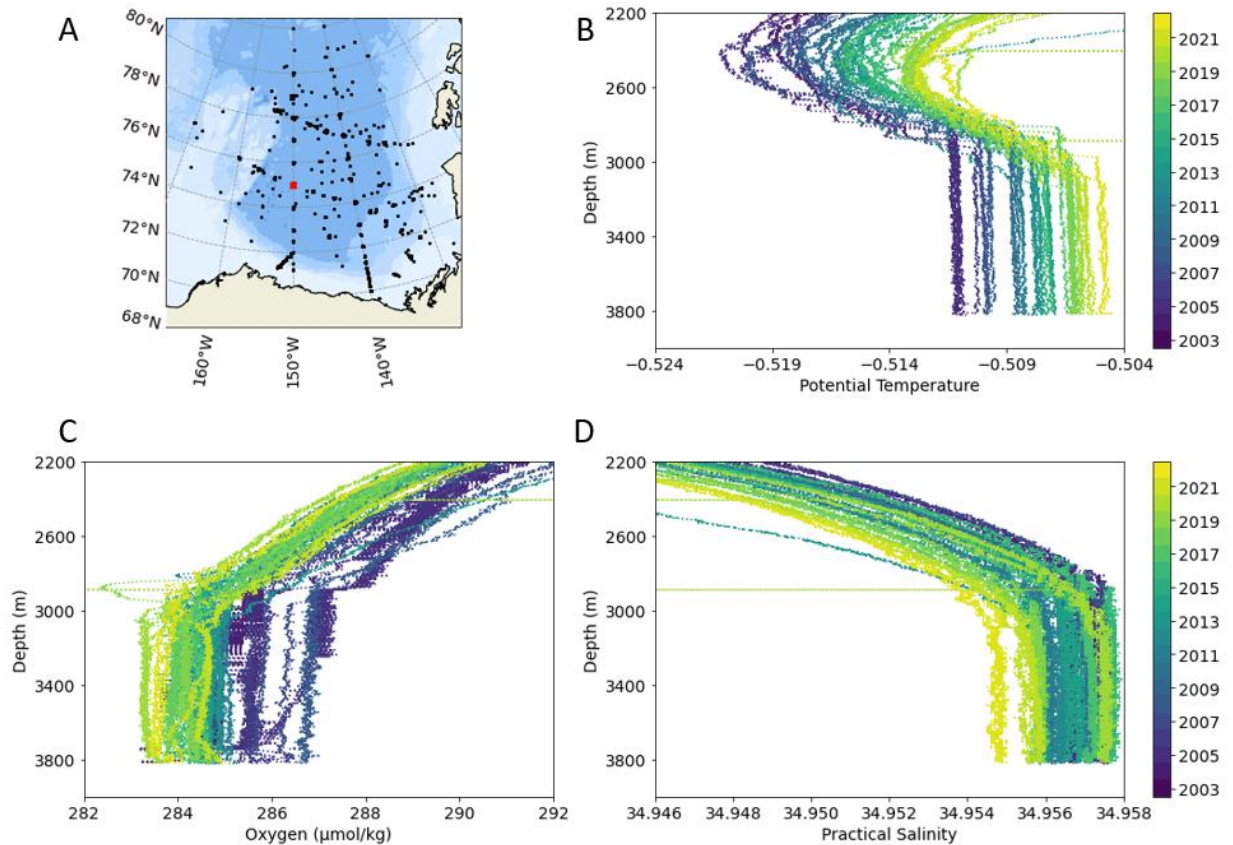


Figure 4. (A) Map showing the locations of all cruise profiles as black dots. The location 75°N, 150°W is the red “x,” which was used to create graphs (B)-(D). (B) Potential temperature, (C) dissolved oxygen, and (D) practical salinity profiles at 75±1°N, 150±1°W from 2003-2022.

3.2 Spatial variations

The structure of the transition layer varies across the CB. In general, the staircase structure occurs most often and most distinctly in the basin interior compared to the edges near the shelves and is warmer and shallower near the shelves than in the interior. Additionally, these staircases are more consistent and are found at shallower depths in the East CB than the West CB. The data also show that the transition layers in the East tend to span a greater range of potential temperatures than in the West, leading to slopes of larger magnitude. An example of these trends is seen in Fig 5.

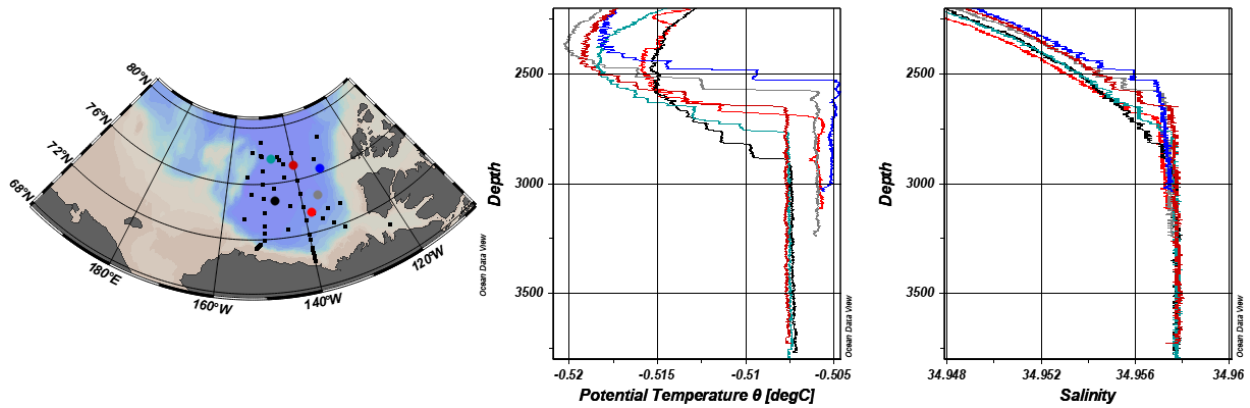
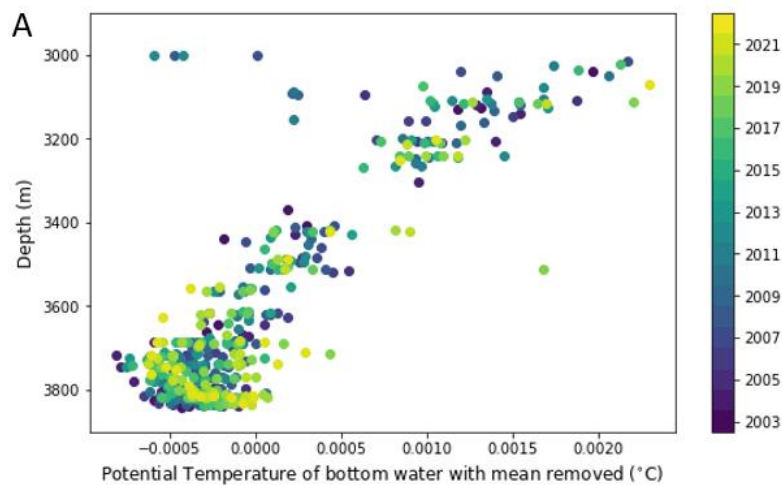


Figure 5. Potential temperature and salinity profiles for select profiles in 2016. The dark blue represents a typical near-shelf profile while the black represents a typical deep basin profile. The teal and grey profiles are representative of typical west and east profiles, respectively.

We can further examine the general spatial trend in the CB deep water by comparing the depth of each cast with its average potential temperature, salinity, and dissolved oxygen variation from its yearly average. From Fig. 6, we see that shallower profiles (i.e., profiles closer to the shelves) are generally warmer, less saline, and contain less dissolved oxygen than deeper profiles. A least-squares linear regression reveals statistically significant trends in all observed properties: potential temperature decreases with depth at a rate of $(-2.2 \pm 0.1) \times 10^{-6} \text{ } ^\circ\text{C m}^{-1}$, salinity increases with depth at a rate of $(5.5 \pm 0.7) \times 10^{-7} \text{ m}^{-1}$, and dissolved oxygen content increases with depth at a rate of $(7.6 \pm 1.4) \times 10^{-4} \text{ } \mu\text{mol kg}^{-1} \text{ m}^{-1}$.



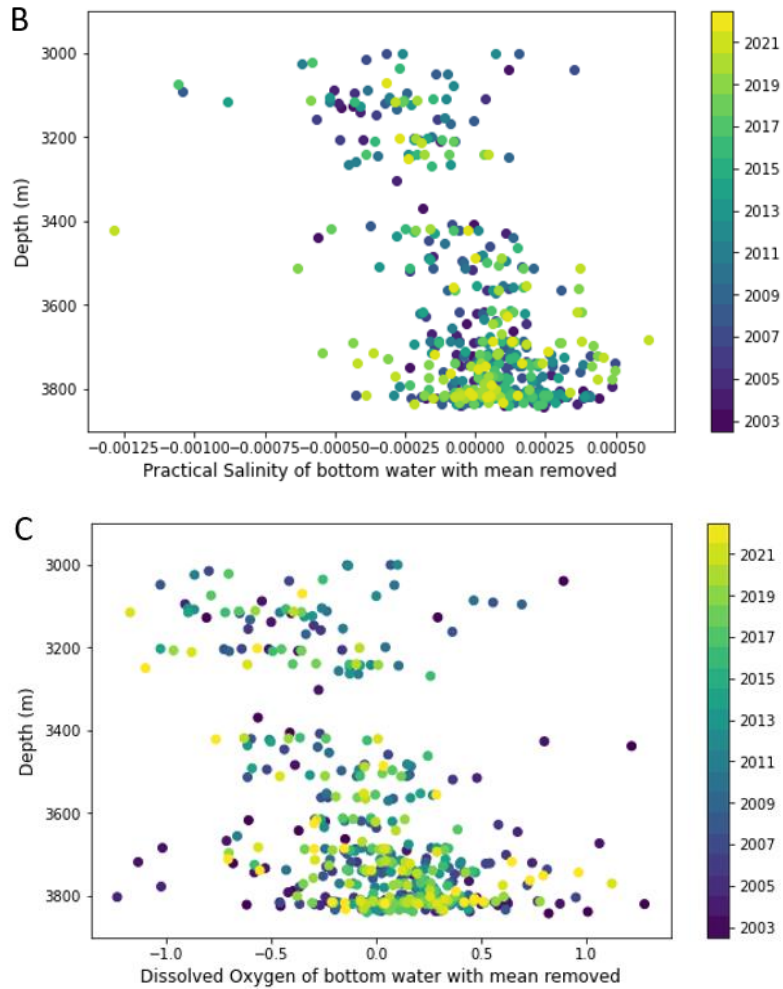


Figure 6. (A) shows a scatter plot of CB bottom water potential temperature versus bottom depth for cruises 2003-2022, showing the increase in bottom water temperature with decreasing bottom depth. The average CB bottom water temperature was subtracted from each profile to remove the warming trend. (B) and (C) are similar scatter plots but for practical salinity and dissolved oxygen respectively.

Now viewing spatial variations within each year of data, salinity sections show slight variations in staircase depth and intensity across the basin. Fig. 7 shows two examples of large disturbances, one in 2013 and one in 2015. These vertical displacements are on the order of ~100m and do not extend further than one station in the section they appear in.

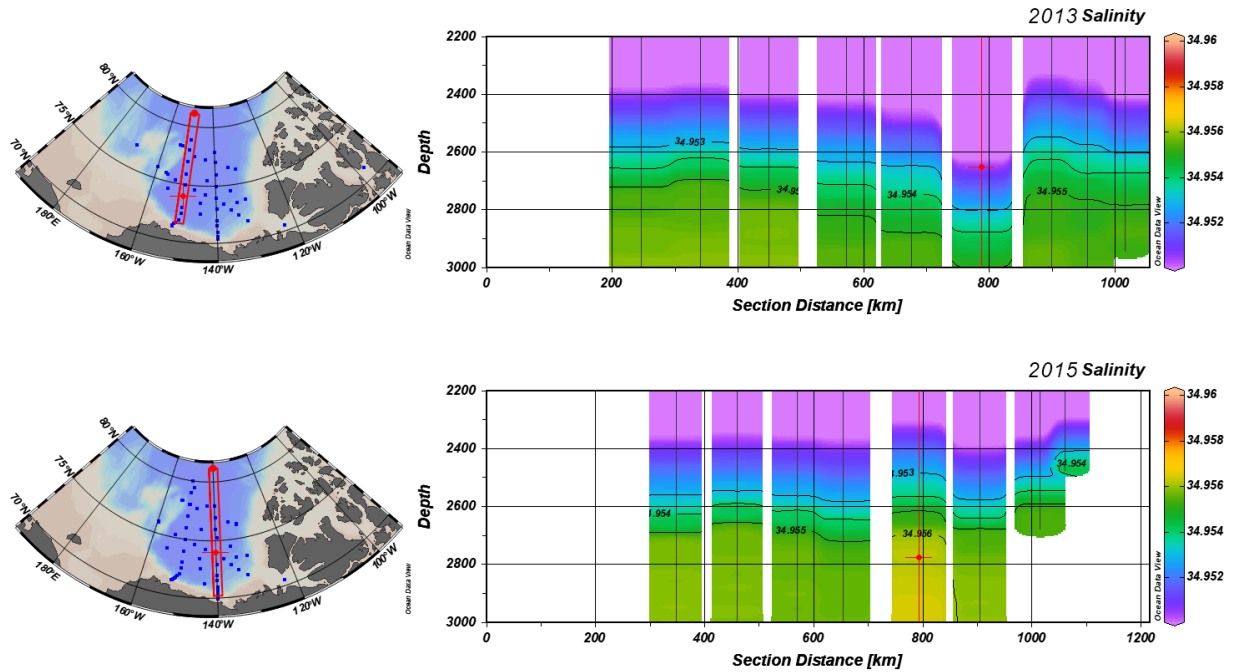


Figure 7. Two different sections at two different years. The 150°W section from 2013 (top) shows a dip in staircase depth while the 140°W section from 2015 (bottom) shows a protrusion in staircase depth.

3.3 Temporal Variations

From specific locations to basin-wide averages, the CB deep water is increasing in potential temperature, decreasing in salinity, and decreasing in dissolved oxygen. Fig. 8 demonstrates the uniform change in potential temperature within the CB bottom water, which is expected given the isolated nature of the water mass and the uniform nature of geothermal heating (Carmack et al., 2012). This knowledge allows us to examine basin-wide changes in CB deep water properties over time.

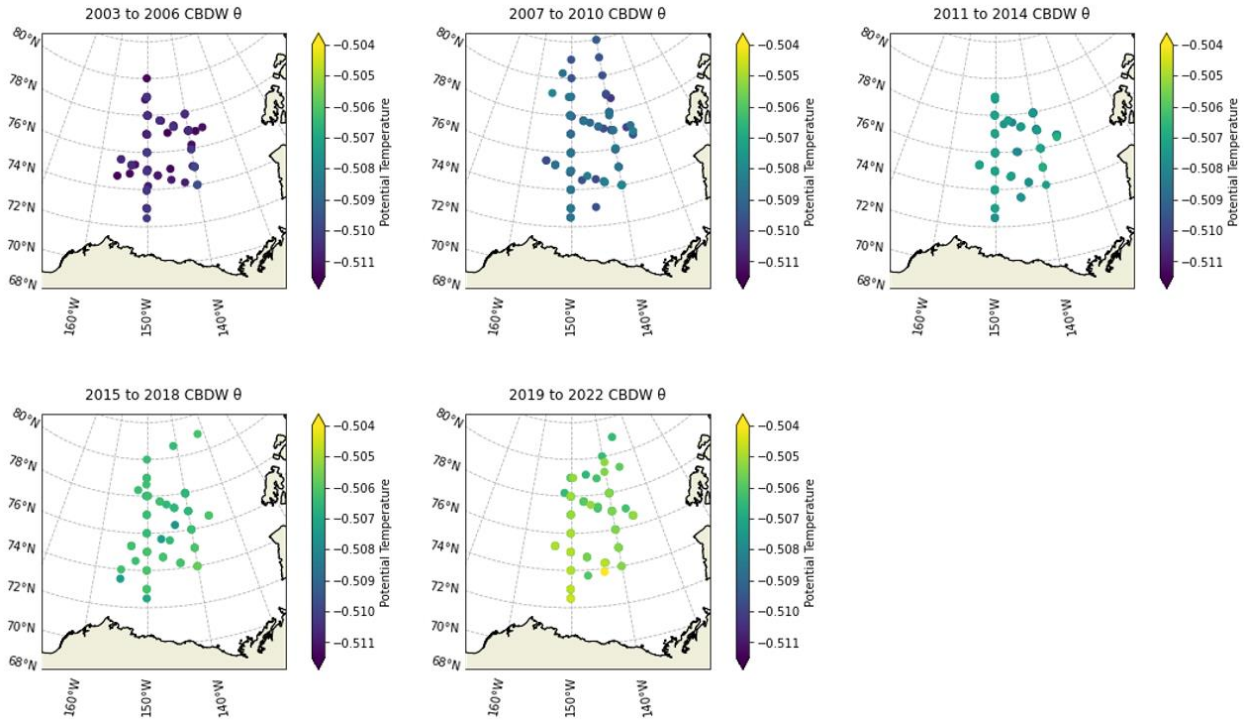


Figure 8. Temperature maps of average CB bottom water potential temperature across the basin in groups of four years.

The time series for average potential temperature, salinity, dissolved oxygen, and AOU across the basin is shown in Fig. 9. By performing a least-squares linear regression on the yearly average potential temperature, practical salinity, dissolved oxygen, and AOU at the depth of T_{\min} and over the CB bottom water, we show that all four properties at both locations have statistically significant linear trends except for practical salinity in the CB bottom water (Table 1). For all properties except practical salinity, the CB bottom water and the water column at T_{\min} experienced the same rate of change from 2003-2022.

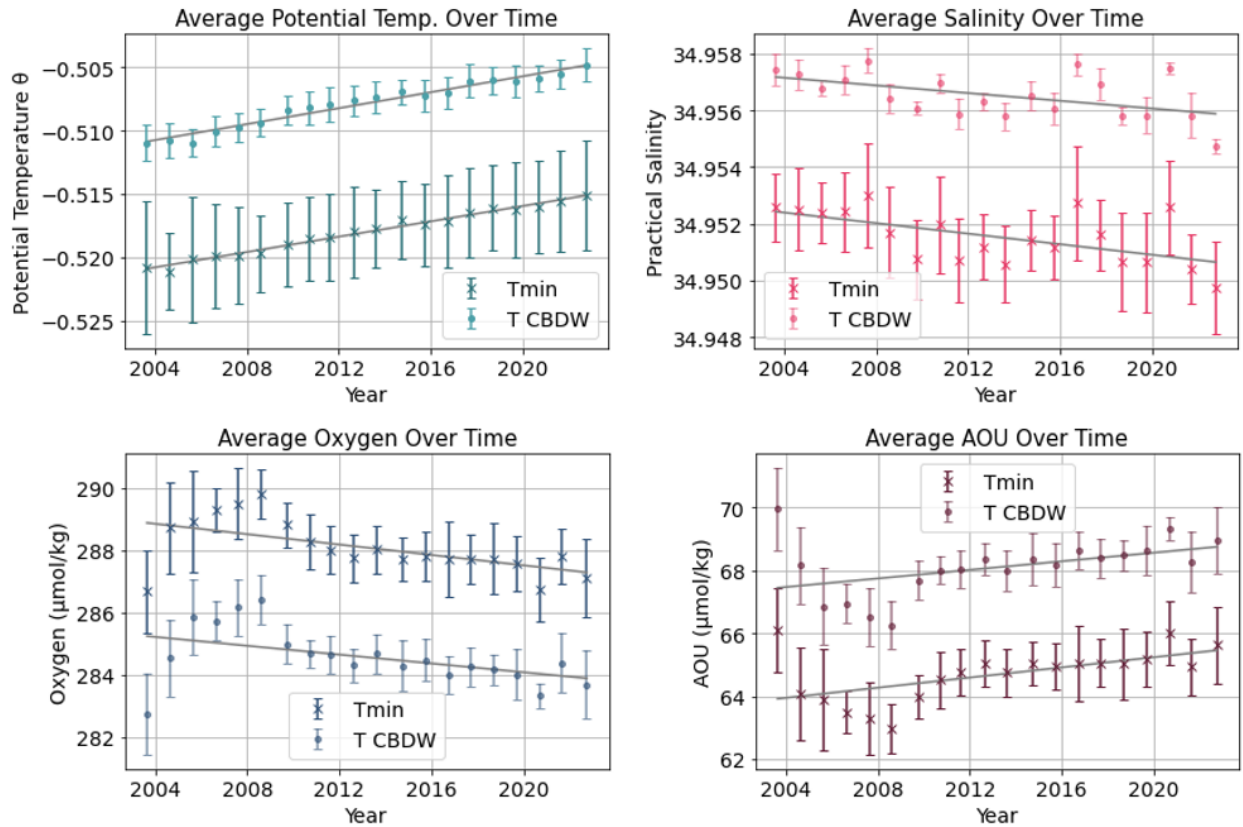


Figure 9. Four plots showing the time series of average potential temperature, practical salinity, dissolved oxygen, and apparent oxygen utilization for 2003-2022 at T_{\min} and in the CB bottom water (written as T CBDW in the legends). Error bars represent two times the standard deviation. Gray lines are the calculated linear trends.

Table 1. Linear trends and 95% confidence intervals for the change in basin-wide average potential temperature, practical salinity, dissolved oxygen, and AOU at the T_{\min} and in the CB bottom water.

	Potential Temp. ($^{\circ}\text{C yr}^{-1}$)	Practical Salinity (yr^{-1})	Dissolved O₂ ($\mu\text{mol kg}^{-1} \text{yr}^{-1}$)	AOU ($\mu\text{mol kg}^{-1} \text{yr}^{-1}$)
T_{\min}	$(3.1 \pm 0.2) \times 10^{-4}$	$(-9.8 \pm 5.2) \times 10^{-5}$	-0.11 ± 0.05	0.11 ± 0.05
CB bottom water	$(3.2 \pm 0.3) \times 10^{-4}$	$(-3.5 \pm 6.6) \times 10^{-5}$	-0.12 ± 0.05	0.11 ± 0.05

Despite the consistency of the overall shape of the CB deep water, the extent of the deep water has changed over time. Analysis of the depth of T_{\min} and the thickness of the CB bottom water layer shows at three locations that the overall thickness of the CB deep water has been

decreasing with time. This trend is most apparent at Location 1 (75°N, 150°W) (Fig. 10), where the T_{\min} is increasing in depth at a rate of $7.5 \pm 4.0 \text{ m yr}^{-1}$ and the CB bottom water is decreasing in thickness at a rate of $-10.4 \pm 3.6 \text{ m yr}^{-1}$.

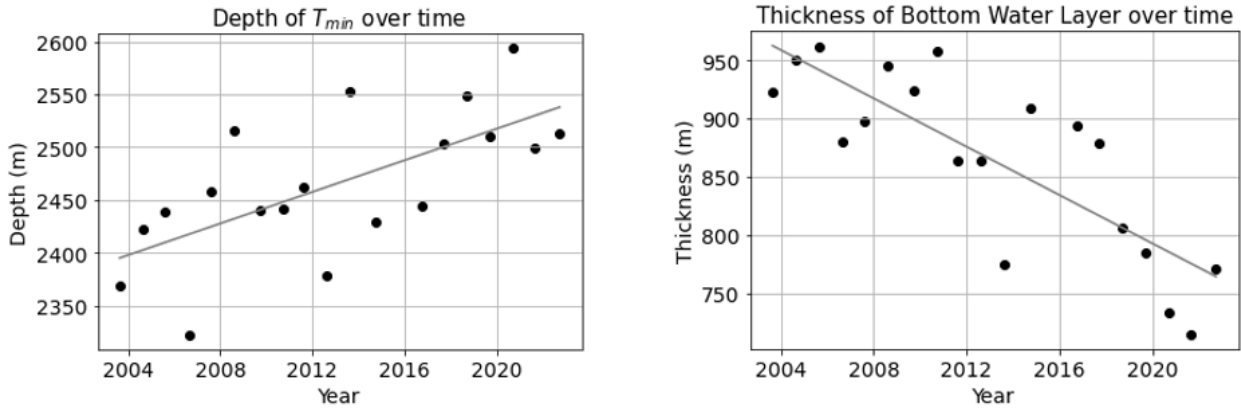


Figure 10. Time series showing the average depth of T_{\min} (left) and the average thickness of the CB bottom water layer (right) at $75 \pm 1^\circ\text{N}$, $150 \pm 1^\circ\text{W}$ from 2003-2022. The gray lines represent calculated linear trends.

3.4 Oxygen in the CB deep water

To better isolate the causes of dissolved oxygen change within the CB deep water, we examine the relationship between O_2sol and dissolved oxygen (Fig. 11). Though the two variables are positively correlated, the scale of O_2sol change is smaller than that of dissolved oxygen, showing that changes in dissolved oxygen are not strongly dependent on changes in O_2sol . Changes in dissolved oxygen are related more closely to changes in AOU instead, and associated implications will be discussed below in the discussion section.

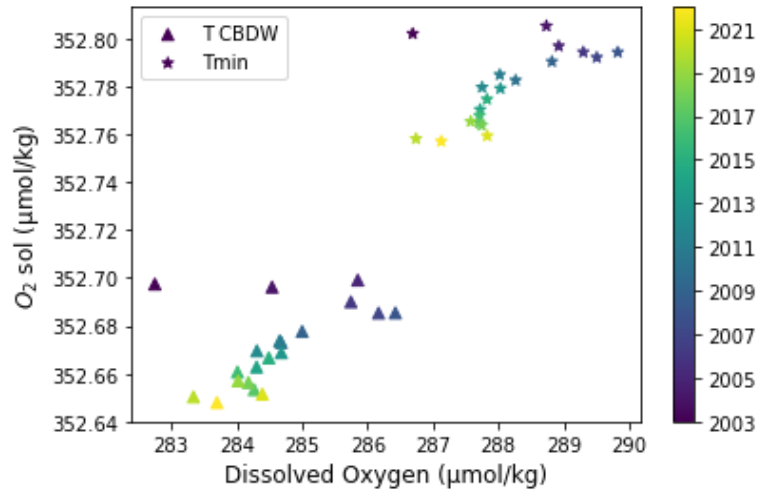


Figure 11. Scatter plot of average dissolved oxygen versus average O₂ sol over the CB bottom water (triangles) and at the location of T_{min} (stars) from 2003-2022.

4 Discussion

4.1 Spatial Characteristics

The spatial characteristics of the CB deep water agrees with the existing literature. As seen in Fig. 4, potential temperature and practical salinity hold their characteristic structure from year to year, showing a persistence of the striking staircase structure of the CB deep water first defined by Timmermans et al. (2003) for now 20 years. The staircase structure was also seen to be more well-defined and deeper in the basin interior than near the shelves, consistent with previous findings by Timmermans et al. (2003) and Carmack et al. (2012). The temperature of the CB bottom water increased with decreasing bottom depth, and the difference in temperature between water with bottom depths of 3000 m and the average CB bottom water ($\sim 0.0020^{\circ}\text{C}$ warmer) matched the value calculated by Carmack et al. (2012). This spatial distribution of temperature is due to shallower layers warming faster in the presence of a uniform heat flux and implies that there is little lateral heat flow (otherwise, all water of the same layer should have the same temperature). The effect of depth on bottom temperature may also help explain how profiles in the eastern CB profiles tend to be warmer and have shallower T_{min} depths than western CB profiles, since there is a more gradual decrease in basin depth at the eastern shelf than the western shelf. On the other hand, salinity decreased with decreasing depth, but the change in value was small (~ 0.0003 less salty at 3000 m than at the bottom). This lack of variation further confirms the lack of ventilation of the CB deep water.

We can now also define a characteristic structure of the CB deep water dissolved oxygen. Seen in Fig. 4, dissolved oxygen profiles show a decrease in oxygen starting before T_{\min} that persists until the transition layer, where the profile has a staircase with decreasing values before arriving at the homogenous bottom layer. The dissolved oxygen staircase mixed layers and interfaces match the thicknesses of the potential temperature and practical salinity profiles, which is expected since the staircase represents laterally-cohesive layers in the water column. When examining the variation in dissolved oxygen across the basin, we found that oxygen concentration decreased with decreasing depth. These variations could be caused by the increase in temperature in shallower waters and/or different organisms living closer to the shelves with higher rates of respiration.

Though the thermohaline structure of the CB deep water is consistent, the depth of the T_{\min} , transition layer, and thickness of the CB bottom water vary slightly across the basin. The vertical displacements identified in salinity sections (such as those shown in Fig. 7) may indicate a dynamically active environment in the deep basin as Timmermans et al. (2007) suggests. In some years, these variations can be drastic, possibly indicating large-scale water transport, such as an eddy. Studies of deep eddies in the Arctic Ocean have detected eddies at depths of 1800 m (Carpenter & Timmermans, 2012) and with thicknesses of 1300 m (Zhao & Timmermans, 2015), so detecting eddy activity in the CB deep water might not be unreasonable.

4.2 *Temporal evolution*

The rates of average potential temperature change across the basin at T_{\min} and the CB bottom water are both $\sim 0.0003 \text{ }^{\circ}\text{C yr}^{-1}$ over 2003-2022. This rate is one ten-thousandth of a degree less than the rate of warming found by Carmack et al., (2012) ($\sim 0.0004 \text{ }^{\circ}\text{C yr}^{-1}$ for both T_{\min} and CB bottom water), which provides further support for the hypothesis that geothermal heat flows vertically upwards from the ocean floor and is then stored in the CB deep water. Additionally, calculations by Carmack et al. (2012) show that a warming rate of $\sim 0.0004 \text{ }^{\circ}\text{C yr}^{-1}$ requires a total geothermal heat flux of $60\text{-}65 \text{ mW m}^{-2}$, a heat flux just within the accepted CB geothermal heat flux range $40\text{-}60 \text{ mW m}^{-2}$ calculated by Langseth et al. (1990). Our slightly lower rate of warming would result in a smaller calculated total geothermal heat flux and would better fit into the accepted range.

The rate of salinity decrease across the basin is $(-9.8 \pm 5.2) \times 10^{-5} \text{ yr}^{-1}$ at T_{\min} and $(-3.5 \pm 6.6) \times 10^{-5} \text{ yr}^{-1}$ for the CB bottom water from 2003-2022. The average practical salinity time series of the CB bottom water did not result in a statistically significant linear trend, so the expected $1 \times 10^{-5} \text{ yr}^{-1}$ decrease in salinity due to double diffusion calculated by Timmermans et al. (2003) can not be confirmed nor denied. Strangely, we found salinity to decrease at T_{\min} , where we would expect no change in salinity at the top of the transition layer if double diffusion were happening (Timmermans et al., 2003). The lack of a clear decreasing trend in the CB bottom water could indicate the replenishment of salinity through shelf drainage of saline plumes, though the variation in the salinity data could also be the result in calibration differences from year-to-year.

We can gain a clearer understanding of ventilation in the CB deep water by observing changes in oxygen. In Fig. 11, we see that dissolved oxygen concentrations were decreasing with decreasing $O_{2\text{sol}}$ from 2003-2022. However, because the overall change in $O_{2\text{sol}}$ ($\sim 0.16 \mu\text{mol kg}^{-1}$) is very small compared to that of dissolved oxygen ($\sim 6 \mu\text{mol kg}^{-1}$), we conclude that changes in dissolved oxygen concentration are not driven by changes in $O_{2\text{sol}}$. Changes in dissolved oxygen must then be related to changes in AOU. In Fig. 9, we see that the AOU at T_{\min} and in the CB bottom water have an equal positive trend of $0.11 \pm 0.05 \mu\text{mol kg}^{-1} \text{ yr}^{-1}$. Positive change in AOU indicates remineralization and respiration, so the CB deep water is likely to be experiencing oxygen consumption through bacterial respiration. Overall, these trends in oxygen data are to be expected for a nonventilated CB deep water – a weak $O_{2\text{sol}}$ to dissolved oxygen connection and a positive trend in AOU shows that the CB deep water is not being refreshed by new water from the surface and reflects the fact that cellular respiration is always happening.

The increase (decrease) in dissolved oxygen (AOU) from 2003-2008 is not captured by the linear trend and may be the result of a change in the CB deep water. Visual inspection of Fig. 9 reveals that there may be similar breaks in the linear trend in potential temperature and practical salinity between 2003-2008 and 2008 onward. The increase in dissolved oxygen and the (visually) greater salinity could be caused by a ventilation event in the CB deep water. Further exploration would be needed to confirm this hypothesis.

4.3 *The decreasing extent of the CB deep water*

An increase in T_{\min} depth and a decrease in CB bottom water thickness from 2003-2022 are seen at all three locations analyzed, demonstrating a decrease in the overall extent of the CB deep water over time. This compression of the CB deep water could be caused by a change in dynamics of the Beaufort Gyre (BG), a clockwise circulation gyre located in the CB. Since 1997, the BG has been in an anticyclonic circulation regime, accumulating freshwater through Ekman downwelling (Proshutinsky et al., 2002). A spin up of the gyre would increase Ekman downwelling and be a potential cause of the height change of the CB.

5 **Conclusions and Directions for Further Research**

This study examined the spatial and temporal changes in the CB deep water using 2003-2022 annual hydrographic survey data. The results from this study and their implications for ventilation rates, heat flows, and other dynamics are as follows:

1. The spatial variation of the CB deep water has been consistent from 2003 to 2022. With decreasing bottom depth, the CB bottom water experiences an increase in potential temperature, a decrease practical salinity, and a decrease in dissolved oxygen. These results confirm previous findings by Timmermans et al. (2003) and Carmack et al. (2012) and is evidence for a lack of lateral heat flow.
2. The CB deep water has warmed at a rate of $\sim 0.0003^{\circ}\text{C yr}^{-1}$ from 2003-2022. This warming rate is only $0.0001^{\circ}\text{C yr}^{-1}$ less than the warming rate found by Carmack et al. (2012) and can be explained by a vertical flow and storage of geothermal heat in the CB deep water.
3. The lack of a statistically significant trend in CB bottom water salinity and a positive trend in AOU both imply a scenario in which the CB deep water is experiencing no ventilation. However, the causes for the increase in dissolved oxygen from 2003-2008 and the unexpected negative trend in T_{\min} salinity are unclear and could indicate changing rates of ventilation over time.
4. The depth of T_{\min} is increasing and the thickness of the CB bottom water is increasing at all three locations. This compression of the CB deep water may be caused by changes in BG dynamics.

While this work extended the results presented by Carmack et al. (2012), further research is necessary to complete the spatial and temporal analysis of the data. First, to gain a better understanding of the ventilation rates of the basin, the increase in dissolved oxygen from 2003 to 2008 and the potential temperature and salinity trends during that time needs to be examined. Additionally, analysis of changes in T_{\min} depth and CB bottom water thickness should be calculated at more locations throughout the basin to better quantify the compression of the CB deep water and its potential causes. Finally, calculations of geothermal heat flux from the $\sim 0.0003^{\circ}\text{C yr}^{-1}$ warming trend need to be completed to confirm the magnitude of heat stored and passing through the CB deep water.

Acknowledgements

This project would not have been possible without the help and guidance of my advisor, Professor Mary-Louise Timmermans. I am so grateful for her time, patience, and understanding throughout these past two semesters and for also introducing me to the EPS (then G&G) major during my first semester at Yale. Additionally, I'm thankful to Ashley Arroyo for sharing her expertise on oxygen and to Madelyn Stewart for her unwavering support and encouragement.

The data were collected and made available by the Beaufort Gyre Exploration Program based at the Woods Hole Oceanographic Institution (<https://www2.whoi.edu/site/beaufortgyre/>) in collaboration with researchers from Fisheries and Oceans Canada at the Institute of Ocean Sciences.

References

- Aagaard, K., & Carmack, E. C. (1994). The Arctic Ocean and climate: A perspective. *Washington DC American Geophysical Union Geophysical Monograph Series*, 85, 5-20.
- Aagaard, K., Swift, J. H., & Carmack, E. C. (1985). Thermohaline circulation in the Arctic Mediterranean seas. *Journal of Geophysical Research: Oceans*, 90(C3), 4833-4846.
- Arroyo, A., Timmermans, M. L., Le Bras, I., Williams, W., & Zimmermann, S. (2023). Declining O₂ in the Canada Basin Halocline Consistent With Physical and Biogeochemical Effects of Pacific Summer Water Warming. *Journal of Geophysical Research: Oceans*, 128(4), e2022JC019418.
- Carmack, E. C., Williams, W. J., Zimmermann, S. L., & McLaughlin, F. A. (2012). The Arctic Ocean warms from below. *Geophysical Research Letters*, 39(7).
- Carpenter, J. R., & Timmermans, M. L. (2012). Deep mesoscale eddies in the Canada Basin, Arctic Ocean. *Geophysical Research Letters*, 39(20).
- Garcia, H. E., & Gordon, L. I. (1992). Oxygen solubility in seawater: Better fitting equations. *Limnology and oceanography*, 37(6), 1307-1312.
- Koeve, W., & Kähler, P. (2016). Oxygen utilization rate (OUR) underestimates ocean respiration: A model study. *Global Biogeochemical Cycles*, 30(8), 1166-1182.
- Langseth, M. G., A. H. Lachenbruch, and B. V. Marshall (1990), Geothermal observations in the Arctic region, in *The Geology of North America*, vol. L, *The Arctic Ocean Region*, edited by A. Grantz, L. Johnson, and J. F. Sweeney, pp. 133–151, Geol. Soc. of Am., Boulder, Colo.
- McLaughlin, F. A., E. C. Carmack, S. Zimmermann, D. Sieberg, L. White, J. Barwell-Clarke, M. Steel, and W. K. W. Li (2008), Physical and chemical data from the Canada Basin, August 2004, *Can. Data Rep. Hydrogr. Ocean Sci.* 140, Fish. and Oceans Can., Ottawa, Ont., Canada.
- Proshutinsky, A., Bourke, R. H., & McLaughlin, F. A. (2002). The role of the Beaufort Gyre in Arctic climate variability: Seasonal to decadal climate scales. *Geophysical Research Letters*, 29(23), 15-1.
- Schlosser, P., Kromer, B., Ekwurzel, B., Bönisch, G., McNichol, A., Schneider, R., ... & Swift, J. H. (1997). The first trans-Arctic 14C section: comparison of the mean ages of the deep waters in the Eurasian and Canadian basins of the Arctic Ocean. *Nuclear Instruments and*

Methods in Physics Research Section B: Beam Interactions with Materials and Atoms, 123(1-4), 431-437.

Timmermans, M. L., Garrett, C., & Carmack, E. (2003). The thermohaline structure and evolution of the deep waters in the Canada Basin, Arctic Ocean. *Deep Sea Research Part I: Oceanographic Research Papers*, 50(10-11), 1305-1321.

Timmermans, M. L., Melling, H., & Rainville, L. (2007). Dynamics in the deep Canada Basin, Arctic Ocean, inferred by thermistor chain time series. *Journal of physical oceanography*, 37(4), 1066-1076.

Zhao, M., & Timmermans, M. L. (2015). Vertical scales and dynamics of eddies in the Arctic Ocean's Canada Basin. *Journal of Geophysical Research: Oceans*, 120(12), 8195-8209.

Appendix

Anomalous Data

Due to instrument error or other issues, the following adjustments were made:

- Year 2020, cast 15: two anomalous peaks identified in the CB deep water portion of the profile were skipped when taking potential temperature, salinity, and oxygen averages.
- Year 2020, cast 43: started the bottom of the profile at 3625.197 m to avoid noise.
- Year 2005, cast 15, 17: removed from oxygen calculations because of bad data.
- Year 2008, cast 10, 21, 22: removed from oxygen calculations because of bad data.
- Year 2015, cast 11: removed from oxygen calculations because of bad data.
- Year 2018, cast 59: removed from oxygen calculations due to being an anonymously low oxygen profile compared to other casts that year.